



ELSEVIER

New Astronomy 6 (2001) 197–213

New Astronomy

www.elsevier.nl/locate/newast

The potential of the variable DA white dwarf G117–B15A as a tool for fundamental physics

Alejandro H. Córscico^{1,a}, Omar G. Benvenuto^{2,a}, Leandro G. Althaus^{3,a}, Jordi Isern^{4,b},
Enrique García-Berro^{4,c,*}

^a*Facultad de Ciencias Astronómicas y Geofísicas, Universidad Nacional de La Plata,
Paseo del Bosque S/N, (1900) La Plata, Argentina*

^b*Institut de Ciències de l'Espai, C.S.I.C., Edifici Nexus, Gran Capità 2-4, 08034 Barcelona, Spain*

^c*Departament de Física Aplicada, Universitat Politècnica de Catalunya,
Jordi Girona Salgado S/N, Mòdul B-4, Campus Nord, 08034 Barcelona, Spain*

Received 20 December 2000; received in revised form 29 March 2001; accepted 29 March 2001

Communicated by K. Nomoto

Abstract

White dwarfs are well studied objects. The relative simplicity of their physics allows one to obtain very detailed models which can be ultimately compared with their observed properties. Among white dwarfs there are specific classes of stars, known as ZZ-Ceti objects, which have a hydrogen-rich envelope and show periodic variations in their light curves. G117–B15A belongs to this particular set of stars. The luminosity variations have been successfully explained as due to *g*-mode pulsations. G117–B15A has recently claimed to be the most stable optical clock ever found, being the rate of change of its 215.2 s period very small: $\dot{P} = (2.3 \pm 1.4) \times 10^{-15} \text{ s s}^{-1}$, with a stability comparable to that of the most stable millisecond pulsars. The rate of change of the period is closely related to its cooling timescale, which can be accurately computed. In this paper we study the pulsational properties of G117–B15A and we use the observed rate of change of the period to impose constraints on the axion emissivity and thus, to obtain a preliminary upper bound to the mass of the axion. This upper bound turns out to be $4 \cos^2 \beta \text{ meV}$ at the 95% confidence level. Although there are still several observational and theoretical uncertainties, we conclude that G117–B15A is a very promising stellar object to set up constraints on particle physics. © 2001 Published by Elsevier Science B.V.

PACS: 95.30.C; 97.10.S; 97.20.R

Keywords: Elementary particles; Stars: oscillations; White dwarfs

*Corresponding author.

E-mail addresses: acorsico@fcaglp.fcaglp.unlp.edu.ar (A.H. Córscico), obenvenuto@fcaglp.fcaglp.unlp.edu.ar (O.G. Benvenuto), althaus@fcaglp.fcaglp.unlp.edu.ar (L.G. Althaus), isern@ieec.fcr.es (J. Isern), garcia@fa.upc.es (E. García-Berro).

¹Fellow of the Consejo Nacional de Investigaciones Científicas y Técnicas (CONICET).

²Member of the Carrera del Investigador Científico, Comisión de Investigaciones Científicas de la Provincia de Buenos Aires (CIC).

³Member of the Carrera del Investigador Científico, Consejo Nacional de Investigaciones Científicas y Técnicas (CONICET).

⁴Institut d'Estudis Espacials de Catalunya.

1384-1076/01/\$ – see front matter © 2001 Published by Elsevier Science B.V.

PII: S1384-1076(01)00055-0

1. Introduction

As already pointed out in the excellent review of Raffelt (2000), astrophysical and cosmological arguments and observations have become a well-known tool to obtain empirical information or constraints on existing or hypothetical elementary particles. One of the most important reasons for this is that the dense environment of stars is potentially a powerful source of low-mass weakly interacting particles. Since these particles subsequently escape from the star this mechanism constitutes a sink of energy that ultimately modifies the stellar lifetimes, thus allowing a comparison with the observed lifetimes. This is particularly useful since, as it is well known, the different non-standard theories leave open the possibility that several exotic particles (like axions or gravitons) could exist. Moreover, for several of these particles there are not yet laboratory experiments in the relevant mass range that could eventually impose tight constraints on their existence.

Among other weakly interacting massive particles, axions are the most promising candidates for non-baryonic dark matter and therefore, a great deal of attention has been paid to these particles. However, the window where axions are viable dark matter candidates is progressively getting smaller (Bergström, 2000). Axions were proposed more than 20 years ago as a solution to the strong CP problem (Peccei and Quinn, 1977), and have a small mass $m_{\text{ax}} = 0.60 \text{ eV} 10^7 (\text{GeV}/f_a)$, where f_a is the Peccei–Quinn scale. Thus, the phenomenology of axions is determined by only one number (f_a), the scale of symmetry breaking. There are two types of axion models: the KVSZ model (Kim, 1979) and the DFSZ model (Dine et al., 1981). In the KVSZ model, axions couple to hadrons and photons whereas in the DFSZ model, axions also couple to charged leptons. The coupling strengths depend on the specific implementation of the Peccei–Quinn mechanism through dimensionless coupling constants. Both models do not set any constraints on the value of f_a and therefore, the limits on the mass of the axion must be obtained from experimental tests. The mass of axion has been constrained by laboratory searches but, to date, there are few constraints coming from accelerator tests in the relevant mass range (Raffelt, 2000).

Given this situation, stars and more specifically, our Sun, has been widely used to set up constraints on the mass of the axion. Several experiments to detect solar and galactic axions have been done (Sikivie, 1983; Lazarus et al., 1992) or are currently under way (van Bibber et al., 1994; Matsuki et al., 1996; Hagmann et al., 1998). Until now these experiments have failed to detect axions and consequently, their existence is still an attractive but somehow speculative hypothesis. The most tight constraints to the mass of the axion available nowadays come mostly from astrophysical arguments and allow for a mass range between 10^{-2} and 10^{-5} eV. To be precise, most of the astrophysical limits are on the interaction strength of axions either with photons — through the Primakov conversion ($\gamma \leftrightarrow a$) in the electric field of electrons and nuclei — with electrons — through the Compton ($\gamma + e^- \rightarrow e^- + a$) and Bremsstrahlung ($e^- + (A, Z) \rightarrow e^- + (A, Z) + a$) processes — or with nucleons. Examples of these astrophysical arguments on the coupling strengths are the following (see Raffelt, 2000, for an extensive review). The coupling strength of axions to photons has been restricted through helioseismological constraints on solar energy losses (Degl’Innocenti et al., 1997), the red supergiant Betelgeuse (Carlsson, 1995), or the dynamics of the explosion of supernova SN1987a (Burrows et al., 1990). In the DFSZ model this leads to an upper limit on the mass of the axion of $m_{\text{ax}} \lesssim 0.4$ eV. On its hand the coupling strength of axions to electrons within the DFSZ model is defined using a dimensionless coupling constant $g_{\text{ae}} = 2.83 \times 10^{-11} m_{\text{ax}} / \cos^2 \beta$, where $\cos \beta$ is a model-dependent parameter that it is usually set equal to unity. The most restrictive bounds on this coupling strength come from the delay of helium ignition in low-mass red giants (Raffelt and Weiss, 1995) and give an upper limit of $m_{\text{ax}} \cos^2 \beta \lesssim 0.01$ eV. Finally, the axion-nucleon coupling strength has been mostly restricted by the SN1987a energy-loss arguments (Keil et al., 1997).

Very recently, Domínguez et al. (1999b) have used Asymptotic Giant Branch (AGB) stars as promising astroparticle laboratories. They concluded that the characteristics of the thermal pulses ensuing after the exhaustion of He at the core are modified by the inclusion of axion emission and that the mass of the carbon–oxygen degenerate core is much lower

when axion losses are taken into account. AGB stars are supposed to be the progenitors of white dwarfs and, therefore, white dwarfs are as well excellent candidates to test the existence of several weakly interacting massive particles. This was recognized early by several authors (see, for instance Raffelt, 1996). There is, however, another important reason for this: white dwarfs are well studied stellar objects since the relative simplicity of the physics governing their evolution at moderately high effective temperatures (say $T_{\text{eff}} \gtrsim 6000$ K) allows one to obtain very detailed models which can be satisfactorily compared with their observed properties. Among white dwarfs there is one specific class of stars, known as ZZ-Ceti objects, which have a hydrogen-rich envelope (thus being classified as DA white dwarfs) and show periodic variations in their light curves. G117–B15A belongs to this particular set of stars. The observed periods of pulsation are 215.2, 271 and 304.4 s together with harmonics and linear combinations of the quoted periods, being the dominant pulsation mode the 215.2 s mode. The luminosity variations have been successfully explained as due to g -mode pulsations. G117–B15A has been recently claimed to be the most stable optical clock ever found, being the rate of change of the 215.2 s period very small: $\dot{P} = (2.3 \pm 1.4) \times 10^{-15} \text{ s s}^{-1}$, with a stability comparable to that of the most stable millisecond pulsars (Kepler et al., 2000). The rate of change of the period is closely related to its cooling timescale, which can be accurately computed, thus offering a unique opportunity to test any additional (or hypothetical) sink of energy. This fact was first recognized by Isern et al. (1992), who derived an upper bound to the mass of the axion of 8.7 meV (assuming $\cos^2 \beta = 1$) by using a simplified model and comparing the observed and computed rate of change of the period of the 215.2 s mode.

In this paper we use the observational characteristics of the pulsating white dwarf G117–B15A to obtain an upper limit to the mass of the axion and we show that pulsating white dwarfs are powerful tools for constraining the mass of any hypothetical elementary particle. The paper is organized as follows. In Section 2 we explain our input physics and how the models are computed. In Section 3 we briefly summarize the observational properties of G117–B15A and we discuss the observational un-

certainties of the relevant parameters. In Section 4 we extensively discuss the mode identification procedure and the theoretical uncertainties due to our incomplete knowledge of the adopted input physics and we compare our results with those of other authors. In Section 5 we compute the effects of introducing the axion emissivity in our calculations and we use the observed properties of G117–B15A to impose constraints to the mass of the axion. Finally in Section 6 we summarize our conclusions.

2. Our input physics and the method of calculation

In order to compute the g -modes of the white dwarf models described in this paper, we have used our evolutionary-pulsational code as described in Córscico and Benvenuto (2001). Briefly, both the evolutionary and the pulsational codes are written following a finite differences scheme and the solutions are reached by means of Newton–Raphson iterations; such a method is well known in stellar astrophysics and it is usually referred to as the Henyey method. The evolutionary code contains very detailed physical ingredients. Among others perhaps the most important are: an updated version of the equation of state of Magni and Mazzitelli (1979), and the radiative OPAL opacities (see Rogers and Iglesias, 1998, for an excellent review). Conductive opacities, neutrino emission by several processes, and other physical ingredients are included as well. For more details, the reader is referred to Benvenuto and Althaus (1998) and references therein. On its hand, the pulsational part of the code solves the equations for linear non-radial stellar pulsations in the adiabatic approximation (Unno et al., 1989).

Briefly, non-radial g -modes are a subclass of spheroidal modes whose main restoring force is gravity. These modes are characterized by low oscillation frequencies (long periods) and by a displacement of the stellar fluid essentially in the horizontal direction. For a spherically symmetric star in the linear approximation, a g -mode can be represented as a standing wave of the form $f'_{k,l,m}(r, \theta, \phi, t) = g'_{k,l,m}(r) Y_l^m(\theta, \phi) e^{i\sigma_{k,l,m} t}$, where the symbol “'” indicates a small Eulerian perturbation of a given

quantity f (like the pressure). On their hand, $Y_l^m(\theta, \phi)$ are the corresponding spherical harmonics. Physically, l is the number of nodal lines in the stellar surface and m is the number of such nodal lines in longitude. In absence of any physical agent able to remove spherical symmetry (like magnetic fields or rotation), the eigenfrequencies $\sigma_{k,l,m}$ are dependent upon l but are $2l + 1$ times degenerate in m . Finally, $g'_{k,l,m}(r)$ is the radial part of the eigenfunctions, which for realistic models must be computed numerically together with $\sigma_{k,l,m}$. The index k (known as the radial order of the mode) represents, in the frame of simple stellar models (like those of white dwarf stars which we shall study below), the number of nodes in the radial component of the eigenfunction. For g -modes, the larger the value of k is the longer the oscillation period. For a detailed description of non-radial oscillations in stars, see the textbook by Unno et al. (1989).

Our aim is to compute the eigenmodes and particularly the values of $\sigma_{k,l,m}$ during the evolution of a given stellar object. Now, let us describe how our pulsation and evolutionary codes work together. Firstly, an interval in effective temperature is chosen (hereafter referred to as the T_{eff} -strip), as well as the frequency window to be scanned. The evolutionary code computes self-consistently the white dwarf cooling up to the moment when it reaches the blue (hot) edge of the T_{eff} -strip. Then, the program calls the pulsation routine and begins to scan for the pulsating modes. When a mode is found, the code generates an approximate solution which is improved iteratively. Then, such solution is tested and if necessary, the meshpoint distribution is refined. The mode is again iterated until satisfactory convergence is reached and then it is stored with the aim of being employed later as an approximate solution for the next stellar model of the sequence. This procedure is repeated until the relevant frequency window is fully covered. At this point we have finished the computation of all the modes of the first model belonging to the T_{eff} -strip and the structure of each one is now in the computer memory. Then, the evolutionary code generates the next stellar model and the code calls the pulsation routine again. Now, the previously stored modes are taken as an input to the iterative scheme to approximate the modes of this subsequent stellar model. Again, the solution is iterated, and so

on. The whole procedure is automatically repeated for all the evolutionary models inside the T_{eff} -strip. When the model star evolves out the T_{eff} -strip, the calculation is finished.

An important quantity needed to compute the pulsational spectrum of g -modes is the so-called Brunt–Väisälä frequency, since it basically defines the main pulsational properties of white dwarfs. Due to the compositional changes along the white dwarf structure, there is an important local contribution to this frequency at the chemical interphases, which, in turn, is responsible for the occurrence of mode trapping (that is, modes with a non-negligible amplitude which are confined between two different chemical interphases or one interphase and the surface). In particular, for the case of DA white dwarfs, mode trapping is mainly due to the H–He interphase. The Brunt–Väisälä frequency is usually given by Unno et al. (1989):

$$N^2 = g \left(\frac{1}{\Gamma_1} \frac{d \ln P}{dr} - \frac{d \ln \rho}{dr} \right) \quad (1)$$

where all the symbols have their usual meaning (notice, however, that in this paragraph P stands for the pressure whereas in the rest of the paper it stands for the period of oscillation) and Γ_1 is the first adiabatic exponent. However, and in order to avoid numerical noise, we use the expression given by Brassard et al. (1991):

$$N^2 = \frac{g^2 \rho}{P} \frac{\chi_T}{\chi_\rho} (\nabla_{\text{ad}} - \nabla + B). \quad (2)$$

where χ denotes the partial logarithmic derivative of the pressure with respect to either T or ρ , respectively, and B stands for

$$B = - \frac{1}{\chi_T} \sum_{i=1}^{N-1} \chi_{X_i} \frac{d \ln X_i}{d \ln P} \quad (3)$$

where X_i is the mass fraction of atoms of species i , N is the total number of considered species, and

$$\chi_{X_i} = \left(\frac{\partial \ln P}{\partial \ln X_i} \right)_{\rho, T, \{X_j \neq i\}} \quad (4)$$

Although we do not mean to discuss in depth the comparison of our results with those obtained with other different numerical codes, it is noteworthy that we have thoroughly tested the results of the pulsa-

tional part of the code by comparing our numerical results for the dimensionless eigenvalues with those of the polytropic models of Christensen-Dalsgaard and Mullan (1994), and with the periods corresponding to DA white dwarf models kindly provided by Bradley (2000). To be specific, we have tested our pulsational code with two carbon–oxygen DA white dwarf models of $0.50 M_{\odot}$ and $0.85 M_{\odot}$, the structure of which was computed with the WDEC evolutionary code and its vibrational properties were previously analyzed (Bradley, 1996). We considered a large number of modes, and the differences between our computed periods and those of Bradley (2000) were always smaller than $\approx 0.1\%$. It is also worth noticing that we also tested the influence of the number of meshpoints in the computed eigenvalues. We have found that largely increasing the number of meshpoints in the pulsational calculation does not substantially affect the computed periods. In fact the values changed very slightly ($\ll 0.1\%$).

In order to compute the effects of axion emission, we have incorporated into the evolutionary code the axion emission rates of Nakagawa et al. (1988). Axion emission produces a supplementary energy loss-rate to those that are considered in the standard theory of white dwarf evolution and consequently, axions accelerate the cooling process of white dwarfs. Such an acceleration of the evolution has a direct consequence on the pulsational properties of the object, because it produces an enhanced value of the period derivative of the oscillation modes, \dot{P} (Isern et al., 1992). Of course, due to this extra cooling mechanism, the structure of the white dwarf itself is also affected but in such a way that, as we shall show below, for a given T_{eff} it corresponds a period, P , that is largely independent of the exact value of the axion energy losses. This fortunate fact will allow us to identify an internal structure for G117–B15A independently of the axion emission rates, which largely simplifies our analysis.

3. Some observational characteristics of G117–B15A

G117–B15A is an otherwise typical DA (hydrogen-rich) white dwarf star whose variability was first discovered by McGraw and Robinson (1976). Since

then, it has been monitored almost continuously. The mass and effective temperature of this star have been spectroscopically estimated to be $0.59 M_{\odot}$ and $11,620 \text{ K}$, respectively (Bergeron et al., 1995). More recently, Koester and Allard (2000) have suggested a somewhat lower value for the mass, which appears to be $0.53 M_{\odot}$.

Regarding the variability of this star, its observed periods are (see Kepler et al., 1982) 215.2, 271 and 304.4 s together with harmonics and linear combinations of the quoted periods. Of particular interest for this work is the fact that for the 215.2 s mode it has been possible to find its rate of change, \dot{P} . The first published value of \dot{P} for this star was presented by Kepler et al. (1991). These authors derived an *upper limit* to the rate of change of the period using all the data obtained from 1975 to 1990. This upper limit appeared to be $\dot{P} = (12.0 \pm 3.5) \times 10^{-15} \text{ s s}^{-1}$, much larger than the theoretical predictions. Along this decade several upper limits to the rate of change of the 215.2 s mode have been derived, with values decreasing from a maximum value of $\dot{P} = (3.2 \pm 3.0) \times 10^{-15} \text{ s s}^{-1}$ to a minimum value of $\dot{P} = (1.2 \pm 2.9) \times 10^{-15} \text{ s s}^{-1}$ — see Kepler et al. (2000), for a detailed discussion of the measured values of \dot{P} . Very recently, with a much longer time interval of acquired data, Kepler et al. (2000) re-determined \dot{P} finding a significantly lower value of $\dot{P} = (2.3 \pm 1.4) \times 10^{-15} \text{ s s}^{-1}$, and concluded that, in view of the presently available data, the 215.2 s mode of G117–B15A is perhaps the most stable oscillation ever recorded in the optical band, with a stability comparable to that of the most stable millisecond pulsars. To this regard it is important to realize that, as already mentioned, all the previous determinations of the rate of change of the period were actually upper limits. The reason for this improved accuracy is that as time (squared) passes by the baseline is much larger and, consequently, the error bars decrease, leading to more precise measurements. The important fact however is that all the previous upper limits were consistent each other at the 1σ level and that the last measured value — that of Kepler et al. (2000) — is larger than its corresponding uncertainty yielding, thus, a positive detection and providing a precise measurement of \dot{P} .

An important aspect for the present work is the so-called mode identification. That is, the identifica-

tion of the l and k values corresponding to each observed period. In the case of G117–B15A, the results of Robinson et al. (1995) indicate that the 215.2 s period corresponds to a dipolar mode ($l = 1$). Following the work by Bradley (1998) we shall assume that the other two modes cited above are also dipolar (Brassard et al., 1993; Fontaine and Brassard, 1994), and also that the other periodicities present in the light curve of the star are not associated with actual eigenmodes but are actually due to non-linear effects in the envelope (Brassard et al., 1993). Regarding the radial order of the modes, there exist two possible identifications. Following Clemens (1994) the observed periods are dipolar modes with $k = 2$ (215.2 s), $k = 3$ (271 s) and $k = 4$ (304.4 s). On the other hand, Fontaine et al. (1994) identified these modes as dipolar with $k = 1$ (215.2 s), $k = 2$ (271 s) and $k = 3$ (304.4 s). As we shall show in the following section, our best fit to observations is in accordance with the identifications of Clemens (1994).

4. The internal structure of G117–B15A and the mode identification

For the above-mentioned value of the stellar mass, the theory of stellar evolution predicts an interior rich in carbon and oxygen. The chemical composition of the white dwarf interior as a function of its mass has recently been computed in detail by Salaris et al. (1997). Therefore, for the calculations reported here we shall adopt the chemical profiles obtained by these authors. However, it is worth mentioning that a good deal of work has been done in this regard. In particular, Bradley et al. (1992), among others, have studied the influence of the internal core composition on the structure of white dwarfs and, more specifically in the properties of DA pulsators. More recently, Bradley (1996), and references therein) analyzed several models for DA pulsators and compared his calculations with the observations finding that the chemical composition of the carbon–oxygen core is more likely to be oxygen-rich, in good agreement with the chemical profiles of Salaris et al. (1997). On its hand, Domínguez et al. (1999a,b) have computed updated chemical profiles for the AGB progenitors of carbon–oxygen white dwarfs,

finding chemical stratifications which are very similar to those of Salaris et al. (1997). In this work we have considered as relatively reliable only the chemical composition of the core, which will not be changed unless explicitly stated (however, see below). In order to adjust the pulsational properties of our models to those observed in G117–B15A, we have looked for variations of some details of the chemical profiles and thicknesses of the layers that at present are only poorly determined, like the thickness of the hydrogen outer layer and of the helium layer that is underneath it. To be precise, in looking for such a fitting of the oscillatory properties we have considered the thicknesses of the hydrogen and helium layers as free parameters. There are several theoretical reasons for suspecting that this is a safe procedure, but perhaps the most important one is that the thickness of the hydrogen layer strongly depends on the exact moment at which a white dwarf progenitor departs from the thermally pulsing AGB phase through pulsation-driven mass-loss (see, for instance, Iben, 1984). Regarding the thickness of the helium layer it is important to mention here that, although the theoretical reasons are not so compelling, it is a usual procedure to adopt it as a free parameter as well, and that as it occurs with the hydrogen layer notably influences the cooling rate and, consequently, the rate of change of the period.

Another important quantity is the slope of the chemical profiles of the very outer layers, especially in the helium–hydrogen and carbon–helium interphases. These slopes have a strong influence on the pulsational properties of white dwarfs and especially, in the Brunt–Väisälä frequency, which ultimately can lead to mode trapping (see Brassard et al., 1992). The functional dependence adopted in this work for both composition transition interphases is gaussian. At present it seems possible to look for a more physically sound treatment of these interphase regions since the structure of such zones should be (at least in the case of those that occur in non-strongly degenerate conditions) determined by element diffusion. In fact, diffusion is mainly responsible for expecting the outer layers to be made up of almost pure materials and should also ultimately determine the thickness of such layers. Some authors have incorporated the effects of diffusion in computing white dwarf evolution (see Iben and MacDonald,

1985; Althaus and Benvenuto, 2000) but, to our knowledge, no one has considered yet the effects of diffusion on the pulsational properties of evolving DA white dwarfs. We thus defer such a study to a forthcoming publication.

For our purposes, we have looked for a model with the observed T_{eff} and mass for G117–B15A which *simultaneously* matches the three observed modes as good as possible. After having such a fiducial model, the computation of the theoretical \dot{P} for different values of the axion mass is rather straightforward. In looking for the fiducial model, we have handled some characteristics of the chemical profiles as free (around the values predicted by the standard theory of stellar evolution) and computed the evolution of the resulting model down to the effective temperatures corresponding to that of G117–B15A. Then, we computed the modes to be compared with the observed ones. Given the present uncertainties, the mass of the star and the helium and hydrogen mass fractions were considered to lay in the following intervals: $0.50 \leq M_{\star}/M_{\odot} \leq 0.65$, $-3 \leq \log M_{\text{He}}/M_{\star} \leq -2$, $-8 \leq \log M_{\text{H}}/M_{\star} \leq -4$. Also, as quoted above, we considered different thicknesses for the helium–hydrogen and carbon–helium interphases. Defining the lagrangian mass-coordinate as $q = \log(1 - M_r/M_{\star})$, and Δq as the thickness of the interphase layer, we have considered the following reasonable values: $-0.8 \leq \Delta q_{\text{H-He}} \leq -0.4$ and $-0.8 \leq \Delta q_{\text{He-C}} \leq -0.2$. As it will be clear below, the simultaneous fit of the three modes is a strong condition to be imposed to the slopes of the chemical profile of the interfaces of the star.

In Figs. 1–3 we compare the theoretical periods of the $l = 1$ (dipolar) modes with $k = 1, 2, 3$, and 4 with those observed for G117–B15A. In constructing these figures we have considered models with the observed T_{eff} of 11,620 K, and previously adjusted the rest of the characteristics of the chemical profile to our fiducial values ($\log M_{\text{He}}/M_{\star} = -2$, $\Delta q_{\text{H-He}} = -0.8$, and $\Delta q_{\text{He-C}} = -0.4$) except for the most critical one, which turns out to be the fraction of the stellar mass present in the outermost, pure hydrogen layer. It should be mentioned as well that in computing these fits we have not taken into account the axion emissivity. In the case of the $0.50 M_{\odot}$ models, it is found a rather good fit corresponding to the modes $k = 1, 2$, and 3 with \log

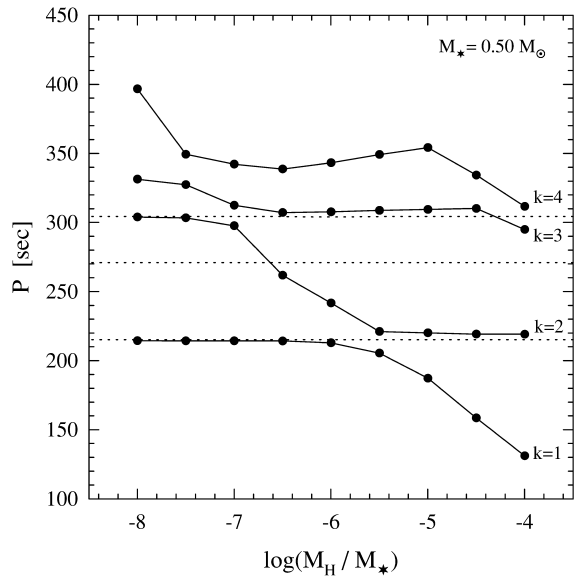


Fig. 1. The period of the dipolar modes $k = 1, 2, 3$, and 4 for a $0.50 M_{\odot}$ model at $T_{\text{eff}} = 11,620$ K as a function of the mass fraction in the outermost hydrogen layer. The rest of the chemical profiles correspond to the best obtained fit (see text for details). The filled dots correspond to the computed models, whereas the short dashed lines represent the observed oscillation periods found in G117–B15A. In this case of a rather low stellar mass, the best fit corresponds to the modes $k = 1, 2$, and 3 with $\log M_{\text{H}}/M_{\star} = -6.6$. For the rest of the computed cases, neither the 215.2 s period nor the two other are well fitted.

$M_{\text{H}}/M_{\star} = -6.6$. In the case of a $0.55 M_{\odot}$ model star we find that the best fit corresponds to the modes with $k = 2, 3$, and 4 and $\log M_{\text{H}}/M_{\star} = -4.0$. Yet there is another acceptable fit for $k = 1, 2$, and 3 and $\log M_{\text{H}}/M_{\star} = -7.0$, although the previously mentioned fit can undoubtedly be considered as much better. In the case of the $0.60 M_{\odot}$ models we have found no satisfactory fit for any of the considered hydrogen mass fractions. Let us also remark at this point that we have also considered the case of models with $0.65 M_{\odot}$, which are not shown for the sake of conciseness.

As explained above, another important free parameter is the thickness of the He-rich layer, since it also influences to a large extent the identification of modes and the cooling rate. To this regard it is important to mention that we have also explored the possibility of thinner helium-rich layers ($\log M_{\text{He}}/M_{\star} < -3.0$) for all the mass values quoted above.

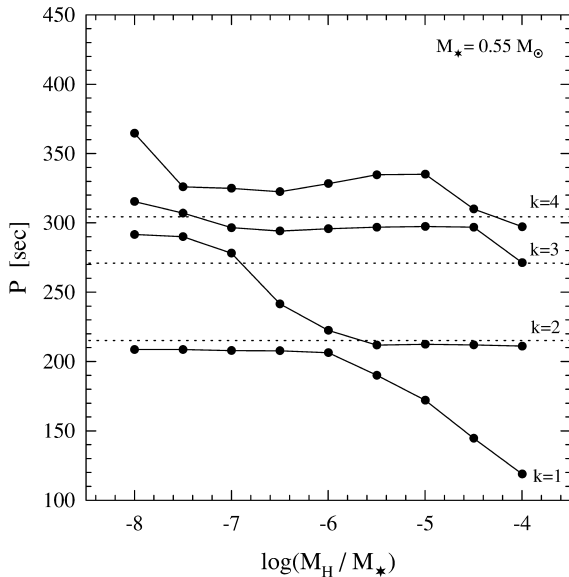


Fig. 2. Same as in Fig. 1, but for the case of a $0.55 M_{\odot}$ model. In this case, the best fit to the observations is found for $k=2, 3, 4$ and $\log M_{\text{H}}/M_{\star} = -4.0$. As this is the best fit to the observations we have found so far, we shall refer to it as the fiducial model. Notice that the amount of hydrogen present in the fiducial model is in very nice agreement with the expectations of the standard theory of stellar evolution. Another acceptable fit is obtained with $k=1, 2, 3$ and $\log M_{\text{H}}/M_{\star} = -7.0$ but the differences between the observed and computed values are far larger than in the previously mentioned case.

Thicker helium layers are quite unlikely according to the most recent AGB studies (Domínguez et al., 1999a,b). In all of these cases the fits to the observations turned out to be significantly worse. Thus we have discarded them and, consequently, we do not show the corresponding fits. Note as well, that besides this being in accordance with the predictions of the theory of stellar evolution it is also in agreement with the results of Bradley (1998).

These results clearly indicate that the mass of G117–B15A should be very close to $0.55 M_{\odot}$ and that the hydrogen mass fraction present in the star should also be close to $M_{\text{H}}/M_{\star} = 10^{-4}$. In fact, the value we derive for the mass of G117–B15A is nicely bracketed by the independent spectroscopic determinations of Bergeron et al. (1995), who obtained $0.59 M_{\odot}$, and of Koester and Allard (2000), who obtained $0.53 M_{\odot}$. It is also worth noticing that our best fit is very similar to the one presented by

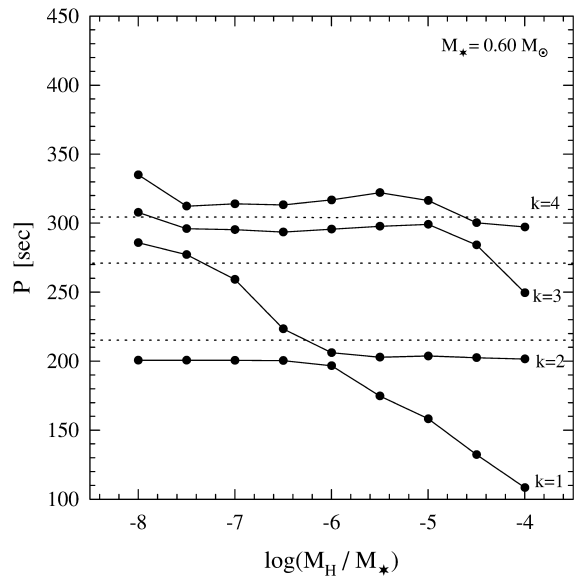


Fig. 3. Same as in Fig. 1, but for the case of a $0.60 M_{\odot}$ model. In this case, we have found that the observations are not well fitted by any of the considered hydrogen mass-fractions. This strongly suggests, in accordance with the findings of other authors (see text), that the mass of this white dwarf is lower than the value considered in this figure.

Bradley (1998) assuming an $l = 1, k = 2$ mode for the 215.2 s period, although this author used a stellar mass of $0.60 M_{\odot}$. Notably, the amount of hydrogen that we have found in G117–B15A is in very nice agreement with the predictions of the standard theory of stellar evolution. The model that provides the best fit to the observations ($M_{\star} = 0.55 M_{\odot}$, $k = 2, 3, 4$ and $\log M_{\text{H}}/M_{\star} = -4.0$) will be hereafter referred to as the fiducial model.

In Fig. 4 we show the profiles of chemical composition of the fiducial model. These profiles are essentially the profiles presented by Salaris et al. (1997) corresponding to the derived mass value of $\sim 0.55 M_{\odot}$. The abundance (by mass fraction) of oxygen in the degenerate core is $\approx 83\%$. Atop the degenerate core there is a partially degenerate helium layer of about 1% of the total mass. Finally, as quoted above, the outermost hydrogen layer embraces $10^{-4} M_{\star}$. It is interesting to note as well that most of the mass of the white dwarf is in the form of oxygen.

Another relevant issue is the precision of the computed periods. In other words, which are the

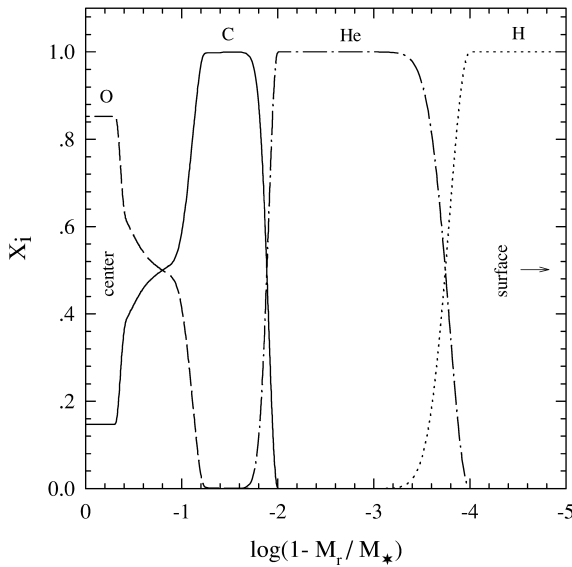


Fig. 4. The internal chemical composition of the white dwarf model that best matches the observed pulsation periods of G117–B15A. This is essentially the profile obtained by Salaris et al. (1997) for a mass value of $0.55 M_{\odot}$. The composition of the white dwarf core is $\approx 83\%$ by mass of oxygen, being the remaining 17% carbon. Atop the degenerate core there is a helium layer of about 1% of the total mass. The outermost hydrogen layer embraces $10^{-4} M_{\star}$, which is in nice agreement with the predictions of the stellar evolution theory. Notice that only the inter-phases between carbon–helium and helium–hydrogen have been tuned to fit the observations. For a discussion of the physical plausibility of such tuning, see text.

typical errors of the theoretical periods of fiducial model when compared to the observational data of G117–B15A? We do not intend here to make sophisticated comparisons, which in fact are possible, but instead, given the discrete nature of our model grid and the small number of periods we are trying to match, we will perform an approximate test. The differences between the observed frequencies and the theoretical ones are 4.63 s (for $k = 2$), 0.58 s (for $k = 3$) and 7.26 s (for $k = 4$), thus giving an average difference of ~ 4 s, which is in good agreement with the results of Bradley (1998). This is a reasonable value, since many of the subtle details of the pulsation calculations can influence the computed periods at several seconds level. There is still another way of estimating the precision of the theoretical periods. Given that we have found that the thickness of the helium layer largely influences

the computed periods and given that we do not get an acceptable fit for thicknesses smaller than $10^{-2} M_{\star}$ we will focus only on the value of the thickness of the outermost hydrogen layer. We define the quantity

$$\psi = \log \sum_{i=1,2,3} (1 - P_i^{\text{theor}} / P_i^{\text{obs}})^2 \quad (5)$$

and we minimize it as a function of M_{H} and M_{\star} . We obtain two local minima: one at $\log(M_{\text{H}}/M_{\star}) = -4.04$ and $M_{\star} = 0.55 M_{\odot}$ and another one at $\log(M_{\text{H}}/M_{\star}) = -6.60$ and $M_{\star} = 0.50 M_{\odot}$. We have chosen the first fit because the mass of the fiducial model is much closer to the spectroscopic mass of G117–B15A. Then we look for the deviations around this minimum and we find that the typical width of the minimum is of the order of 2 s. Since this value is smaller than the previously obtained average value of the differences between the theoretical and the observational data we consider that a reasonable value of the goodness of the fit is ≈ 5 s, which is the value quoted in Table 1.

Now, we are in a good position to study some general vibrational properties of the fiducial model. In particular we will study the dependence of our results on the observational properties (basically the effective temperature and the mass) of G117–B15A. This is important since the observational uncertainties affect the way the theoretical stellar models are compared with the observations and, thus, can affect the upper limit on the mass of the axion which will be derived below. Therefore, we shall explore the effects resulting from varying the above-mentioned characteristics of the model, keeping constant the fiducial chemical profile discussed earlier. As the mode to be employed is the $l = 1$, $k = 2$, we shall hereafter restrict our analysis to such mode. In order to do so, in Fig. 5 we show the period of the $l = 1$, $k = 2$ mode that best represents the observed period

Table 1

Error budget for the period (in seconds) and for the secular rate of change of the period, in units of $10^{-15} \text{ s s}^{-1}$

Source	ΔP	$\Delta \dot{P}$
Mode identification	5	1.0
M_{\star}	6	1.0
$^{12}\text{C}(\alpha, \gamma)^{16}\text{O}$	4	0.1
T_{eff}	2	0.2

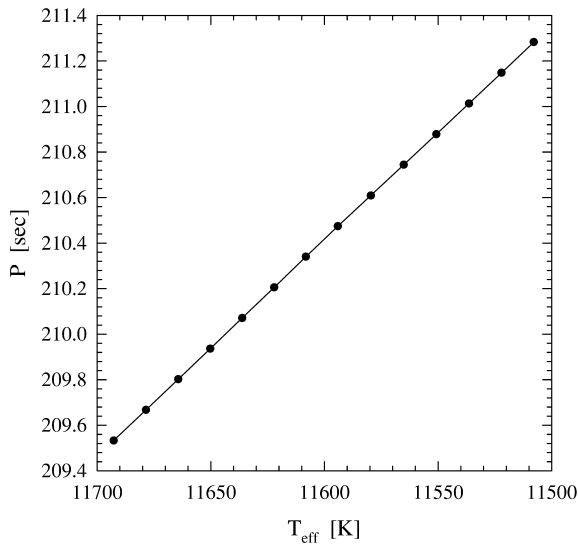


Fig. 5. The period of the $l = 1$, $k = 2$ mode of the fiducial model as a function of T_{eff} . The T_{eff} interval has been chosen to be the corresponding to G117–B15A ± 200 K. Filled dots are the computed models. In this case we have not considered axion emission. Note the monotonic increase in the exact value of the period due to the decreasing temperature of the interior.

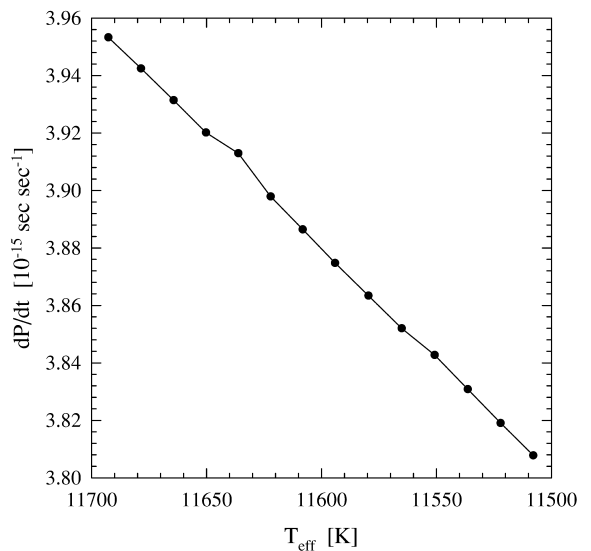


Fig. 6. Same as Fig. 5 but for the temporal derivative of the period corresponding to the $l = 1$, $k = 2$ mode. As in the previous figure we have not considered axion emission. Thus, these results are a lower theoretical limit for the temporal derivative of this mode.

of 215.2 s as a function of the effective temperature in an interval centered around 11,600 K (the observed value for G117–B15A). Note that the monotonic increase in the period of this mode is a direct consequence of the cooling process. On its hand, in Fig. 6 we show the temporal derivative of the period corresponding to the $l = 1$, $k = 2$ mode. It is very important to stress at this point that as in this figure we have not considered yet the possibility of an additional axion cooling mechanism, these results represent the lower theoretical limit for the \dot{P} of this mode. As can be seen in this figures the errors in the determination of the effective temperatures do not induce large errors neither in the mode identification nor in the computed value of \dot{P} .

Now we consider white dwarf models with the fiducial chemical profile and the same T_{eff} and look for the effects of changing the stellar mass. In Figs. 7 and 8 we show the period and its temporal derivative as a function of mass. When one considers models with increasing masses and, hence, with larger gravities the Brunt–Väisälä frequency correspondingly increases (see Eq. (1)). Since all the eigenfrequencies (σ) corresponding to locally non-

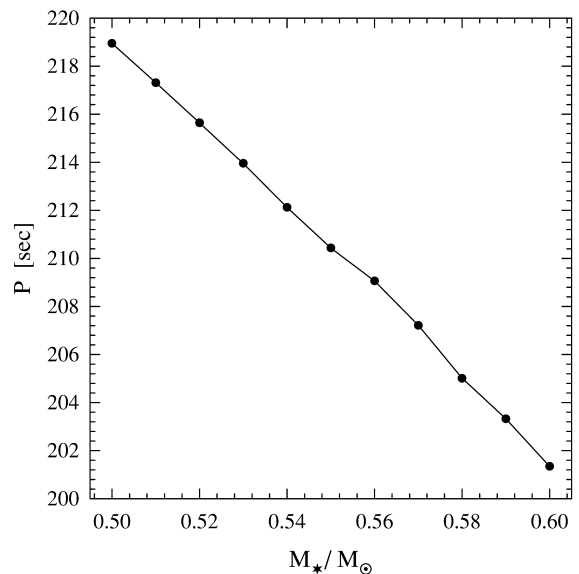


Fig. 7. The $l = 1$, $k = 2$ period for white dwarf models with the chemical profile shown in Fig. 4 and $T_{\text{eff}} = 11,620$ K as a function of their mass. The computed models are depicted with filled dots.

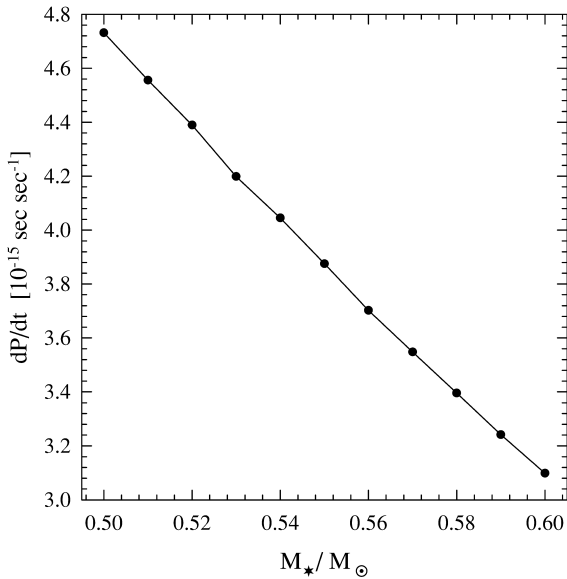


Fig. 8. The temporal derivative of the period of the $l = 1$, $k = 2$ mode for white dwarf models with the chemical profile shown in Fig. 4 and $T_{\text{eff}} = 11,620$ K as a function of their mass. The computed models are depicted with filled dots.

evanescent g -modes verify $\sigma^2 < N^2$ (see Unno et al., 1989) it turns out that all the pulsational spectrum is shifted to larger values, resulting thus in smaller periods. The same behaviour was found by Brassard et al. (1992). Regarding \dot{P} , the larger the mass, the lower the radiating surface and the higher the total heat capacity. As we are at a fixed T_{eff} value, high mass models have smaller luminosities and thus cool slower with a smaller \dot{P} . This can be also understood in terms of the most simple, yet accurate enough for our purposes, cooling law (Mestel, 1952). Within the framework of the Mestel (1952) cooling law the luminosity of a white dwarf is $L \propto M_{\star} T^{7/2}$, where T is the temperature of the nearly isothermal degenerate core, which is a monotonic function of the effective temperature, and the characteristic cooling time turns out to be $\tau_{\text{cool}} = d \ln L / dt \propto (M_{\star} / L)^{5/7}$. Since, to an accuracy similar to that of the Mestel cooling law, the secular rate of change of the period is directly related to the cooling rate we expect:

$$\frac{d \ln P}{dt} \propto - \frac{d \ln T}{dt} \propto \frac{1}{\tau_{\text{cool}}} \propto \left(\frac{L}{M_{\star}} \right)^{5/7} \propto T^{5/2}. \quad (6)$$

Since massive white dwarfs have smaller radii, for

the same effective temperature the luminosity is smaller and, hence, the core temperature is smaller, leading to larger characteristic cooling times and ultimately, to smaller secular changes in the period. In summary, as in the previous set of figures we see that the exact value of P is not significantly altered by the observational errors in the determination of the stellar mass. However, the reverse is true for \dot{P} . In particular, it is convenient to note that the exact value of the period derivative varies by about a 30% in the mass interval 0.5 to 0.6 M_{\odot} , which can be important when comparing with its observed value. Nevertheless, and fortunately, the mode identification performed previously allows us to effectively constrain the mass interval to a much narrower range and, thus, this will not severely affect our results.

Another possible source of uncertainties is the poorly determined rate of the reaction $^{12}\text{C}(\alpha, \gamma)^{16}\text{O}$ that determines the final state of the asymptotic giant branch phase and, thus, the carbon–oxygen stratification inside the core of the newborn white dwarf. Recent experimental data and updated values of the astrophysical S -factor (Arnould et al., 1999) suggest a substantially larger rate than that derived by Caughlan and Fowler (1988), and much closer to the previously value obtained by Caughlan et al. (1985). This yields larger central amounts of oxygen as obtained by Salaris et al. (1997). However, as already noted by these authors, the internal chemical profile of the white dwarf core depends not only on the rate of the $^{12}\text{C}(\alpha, \gamma)^{16}\text{O}$ reaction but on the treatment of convection as well. For instance, Woosley et al. (1993) studied the role of this reaction rate in producing the solar abundance set from stellar nucleosynthesis and concluded that the effective astrophysical S -factor for the energies involved during core helium burning that best reproduces the observed abundances should be closer to the rate given by Caughlan and Fowler (1988). In their models the Ledoux criterion plus an amount of convective overshooting were adopted for determining the extension of the convective regions. On the other hand, the chemical profiles obtained by Salaris et al. (1997) correspond to an enhanced value for the $^{12}\text{C}(\alpha, \gamma)^{16}\text{O}$ reaction rate (Caughlan et al., 1985) and the adoption of the Schwarzschild criterion without any overshooting for the convective instability, which gives an excellent agreement with

the abundances of ^{12}C and ^{16}O found in the ejecta SN1987A (Thielemann et al., 1996). Thus, since we cannot disentangle both effects, the astrophysical constraints are only set on an *effective* cross section for the $^{12}\text{C}(\alpha, \gamma)^{16}\text{O}$ reaction, given the lack of a reliable theory of convection. Here, in assuming the chemical profile computed by Salaris et al. (1997) we have assumed for such a critical reaction the rate given by Caughlan et al. (1985). However, note that a different reaction rate would obviously produce a different carbon–oxygen stratification. It is well known that changes in the internal composition of the white dwarf affect the cooling timescale (and thus the rate of change of the period) because it changes the heat capacity per mass unit. As most of the heat capacity of the star is due to the contributions of the non-degenerate ions, which is inversely proportional to the average atomic number, an enhanced oxygen abundance, like that found by Salaris et al. (1997), implies less heat capacity which, in turn, forces a faster cooling and a larger \dot{P} . Again, in terms of Mestel (1952) cooling law:

$$L \simeq -\frac{dU_{\text{ion}}}{dt} = -C_V M_{\star} \frac{dT}{dt} \propto \frac{1}{A} \quad (7)$$

where C_V is the specific heat and A is the atomic mass number. Clearly, $\tau_{\text{cool}} \propto 1/A$, and consequently the cooling proceeds faster when the oxygen abundance is larger and, according to Eq. (5), the secular rate of change of the period becomes larger. Because of this reason it is interesting to have a quantitative idea of how such an uncertainty in the $^{12}\text{C}(\alpha, \gamma)^{16}\text{O}$ nuclear reaction rate would affect our results. For such a purpose, we have considered different internal carbon–oxygen stratifications keeping the same shape of the fiducial profiles but with different central abundances for the carbon abundance, X_C , ranging from $X_C = 0.0$, to $X_C = 1.0$. Such profiles are shown as dotted lines in Fig. 9 together with the fiducial profile, which is shown as a solid line.

In Fig. 10 we show the period of the $l = 1, k = 2$ mode for a white dwarf model of $0.55 M_{\odot}$ and an T_{eff} of 11,620 K as a function of its central carbon abundance. Notice that changing the carbon profile in the stellar core induces a very modest change of $\approx 4\%$ in the period of the fiducial mode. Such a change in the period is due to the following two reasons. First, the lower the carbon abundance is, the

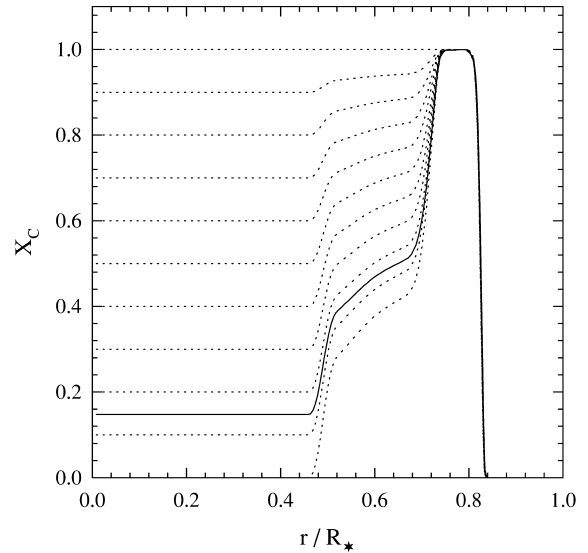


Fig. 9. Profile of the carbon abundance as a function of the stellar radius for models with $X_C = 0.0, 0.1, \dots, 1.0$ central carbon abundances. The short dashed lines correspond to the scaled profiles whereas the solid line correspond to the fiducial carbon profile.

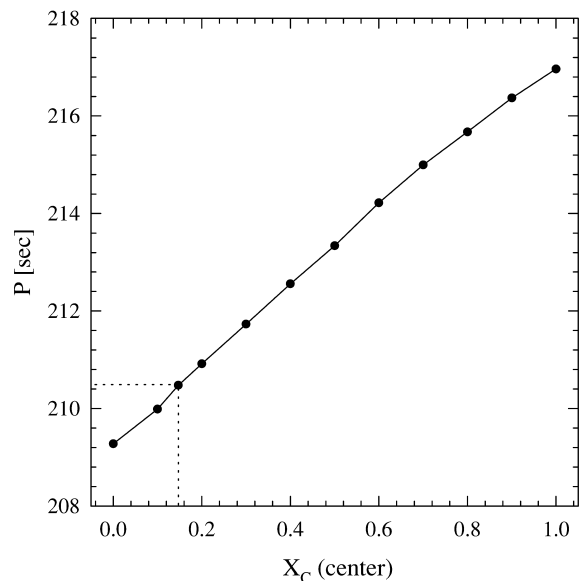


Fig. 10. The period of the $l = 1, k = 2$ mode for white dwarf models of $0.55 M_{\odot}$ and a T_{eff} of 11,620 K as a function of the central carbon abundance. The filled dots represent computed models whereas the short dashed lines indicate the abundance and the period corresponding to the fiducial model.

lower the Coulomb interactions in the stellar plasma are. This, in turn, produces slight changes in the structure of the stellar core. Second, and most important, smaller (larger) carbon central abundances produce steeper (shallower) slopes at the outer boundary of the degenerate core just at the base of the transition zone, leading to different radial configurations of the modes. This, in turn, is important because in our models, the 215.2 s mode has large amplitudes in such an interphase. Consequently, any change in the structure of the interphase will affect the structure of the mode and thus its period. In Fig. 11 we show the temporal derivative corresponding to the modes of the previous figure. Here, as is expected, the lower the central carbon abundance is, the higher the computed \dot{P} is. However, even considering extreme cases, the variation of \dot{P} is very modest: $\approx 7\%$. Thus our results are not severely influenced by our choice of the $^{12}\text{C}(\alpha, \gamma)^{16}\text{O}$ nuclear reaction rate.

After examining all the possible uncertainties a few words are necessary to justify the discrepancy between the measured rate of change of the period of the 215.2 s mode, $\dot{P} = (2.3 \pm 1.4) \times 10^{-15} \text{ s s}^{-1}$, and

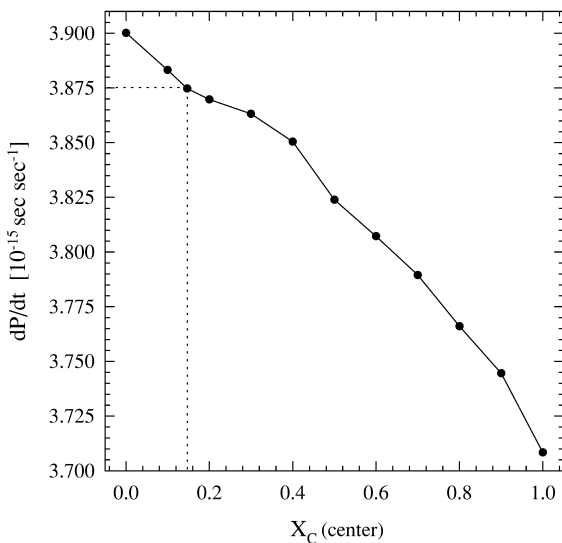


Fig. 11. The temporal derivative of the period of the $l = 1$, $k = 2$ mode for white dwarf models of $0.55 M_{\odot}$ and $T_{\text{eff}} = 11,620 \text{ K}$ as a function of their central carbon abundance. The filled dots represent computed models whereas the short dashed lines indicate the abundance and the temporal derivative of the period corresponding to the fiducial model.

its computed value for the fiducial model, $\dot{P} = 3.9 \times 10^{-15} \text{ s s}^{-1}$. In fact, our computed value for the fiducial model, which is in good agreement with the independent calculations of Bradley (1998), is slightly beyond the formal 1σ error bars. Kepler et al. (1995) carefully discussed the significance and the error bars of all the previous determinations of the upper limits to \dot{P} and argued that there could be some observational artifacts due to the modulation by the nearby frequencies. Moreover, Costa et al. (1999) have recently shown that a realistic estimate of the observational uncertainties must necessarily include the effects of all the periodicities that G117–B15A shows. However, Kepler et al. (2000) already took into account all the periodicities and thus, both the value of \dot{P} and its reported error bars can be considered as safe. But, on the other hand, as discussed by Bradley (1998) and confirmed by the previous study of the theoretical uncertainties performed in this work, a spread of about $\pm 1 \times 10^{-15} \text{ s s}^{-1}$ could be expected from either the mode identification procedure, the precise observational characteristics (like the effective temperature and mass) of G177-B15A and our incomplete knowledge of the physical inputs involved in the calculation of \dot{P} . Table 1 summarizes the approximate theoretical error budget obtained from all the previous calculations, taking into account realistic variations of all the parameters. Finally, it is worth mentioning as well, that another source of uncertainty is the contribution of the proper motion of the G117–B15A (Pajdosz, 1995). With the current estimates of the proper motion and parallax, Kepler et al. (2000) have concluded that the maximum contribution of the proper motion of the star to the observed rate of change of the period is $\dot{P} = (9.2 \pm 0.5) \times 10^{-16} \text{ s s}^{-1}$. We thus conclude that taking into account the theoretical uncertainties, our preferred model could be safely considered as satisfactory and that our value for \dot{P} is fully consistent with the observed rate of change of the period.

5. The effects of an enhanced cooling due to axion emission

Now, we turn our attention to compute the effects of axion emission on the evolutionary timescale of

G117–B15A and its effect on the expected value of \dot{P} for the $l = 1, k = 2$ mode. In order to do this in a self-consistent way we have run an additional set of cooling sequences with different axion masses (and considered the pulsational characteristics in the relevant effective temperature range) for our fiducial model, starting from the same initial conditions used for the models computed without axion emission. This procedure allowed us to take into account the fact that the axion emissivity influences the thermal structure of the white dwarf. This is particularly important since the cumulative effect of axions must have reached an equilibrium value before the model enters into the instability strip in order to avoid an artificial response that would not be representative of the real pulsational characteristics of G117–B15A. In all the evolutionary calculations including the axion contribution, we have verified that the transitory due to the inclusion of axions in the model occurred far before the star cools down to effective temperatures near that of G117–B15A. We have found that, even considering a wide range for the mass of the axion, the period of the $l = 1, k = 2, 3,$ and 4 modes show a very small variation for the

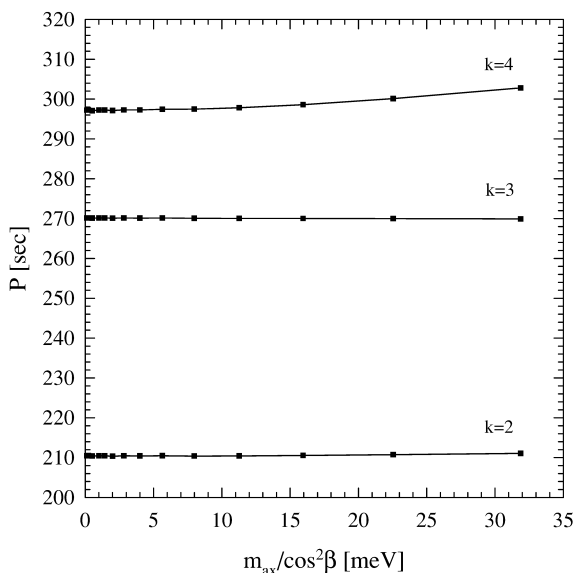


Fig. 12. The periods of the $l = 1, k = 2, 3,$ and 4 modes corresponding to the fiducial model at a T_{eff} of 11,620 K as a function of the axion mass. Notice that, in spite of the acceleration of the cooling process induced by axion emission, the period of these modes do not change significantly.

whole considered interval (see Fig. 12, where we show the values of the period for these modes as a function of the assumed mass of the axion). This is indeed a very fortunate situation that allowed us to employ the procedure of identifying first the structure of the fiducial model without considering axion emission and then to incorporate the axion emissivity. This would have not been the case should we have had to identify a white dwarf structure for each value of the axion mass. In such a case we would have had no fiducial model, thus complicating our analysis enormously.

The fact that the periods of oscillation at a fixed effective temperature are almost independent of the value of axion mass has a simple physical explanation. Axion emission affects the temperature profile in the innermost, strongly degenerate parts of the star. Thus, the structure of the star is only very slightly affected by the axion emissivity. On its hand, the outer layers are partially degenerate and its structure is dependent on the temperature profile. But, for the case we are interested in, such a profile is largely determined by the assumption of a fixed value for the effective temperature. Consequently, as the modes are dependent upon the mechanical structure of the star, the periods are almost unchanged.

In sharp contrast with the small variation of the computed values of the periods of all the modes with the axion emissivity found previously, the value of \dot{P} for the three identified modes is extremely sensitive as it is shown in Fig. 13, where we show the temporal derivative of the period for the same range of the mass of the axion. As an example, for the 215.2 s mode, and for the range of axion masses considered here ($0 \leq m_{\text{ax}}/\cos^2\beta \leq 32$ meV), \dot{P} increases by a factor of about 18. Note that the \dot{P} value corresponding to the mode with $k = 3$ is the smallest one mode in the whole considered axion mass interval. This is due to the fact that this mode is trapped in the outer hydrogen envelope — see Bradley et al. (1992) for a physical justification.

Finally, in Fig. 14 we show the value of \dot{P} of the $l = 1, k = 2$ mode of the fiducial model at $T_{\text{eff}} = 11,620$ K as a function of the mass of the axion. The observational value of Kepler et al. (2000) is also shown as a dashed line. Also shown as dashed lines are the observational errors at 1σ and 2σ and the old value of \dot{P} (Kepler et al., 1991). Now we can look

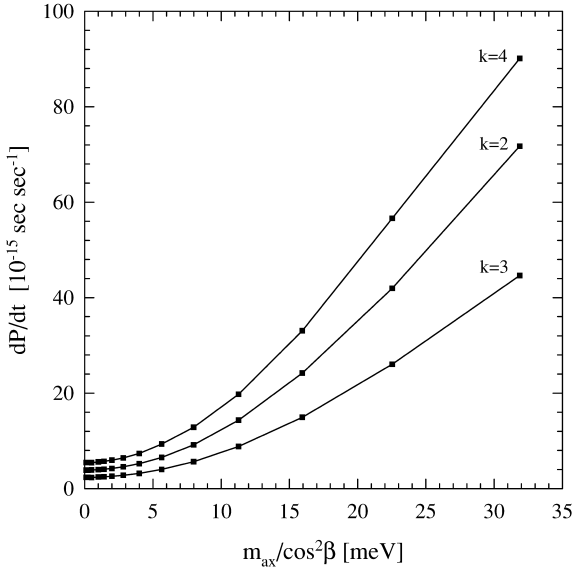


Fig. 13. The derivative of the periods of the $l = 1$, $k = 2, 3$, and 4 modes of the fiducial model at $T_{\text{eff}} = 11,620$ K. Note that for high values of the axion mass, as cooling is strongly accelerated the value of \dot{P} shows a steep increase.

for an upper limit to the axion mass by imposing that the value of \dot{P} should be lower than the observed value plus two times the standard deviation, that is, lower than $5.1 \times 10^{-15} \text{ s s}^{-1}$. Thus, this procedure sets upper limits on the mass of the axion at the 95% confidence level. From a close inspection of Fig. 14 it is clear that for this to be the case, the axion mass must be lower than $3.97 \cos^2 \beta$ meV. This is the main result of the present work. Also, notice that if we consider the old \dot{P} value of Kepler et al. (1991), the upper limit would have been $\approx 10 \cos^2 \beta$ meV in good agreement with the results of Isern et al. (1992).

These results can be easily explained in terms of a very simple model. Isern et al. (1992) found that the observed rate of change of the pulsational period of G117–B15A (\dot{P}_{obs}) and the rate of change of the period given by the models (\dot{P}_{mod}) when axion emission is considered are related through the following expression:

$$\frac{L_{\text{phot}} + L_{\text{ax}}}{L_{\text{phot}}} = \frac{\dot{P}_{\text{obs}}}{\dot{P}_{\text{mod}}} \quad (8)$$

Since we are considering upper bounds at the 2σ

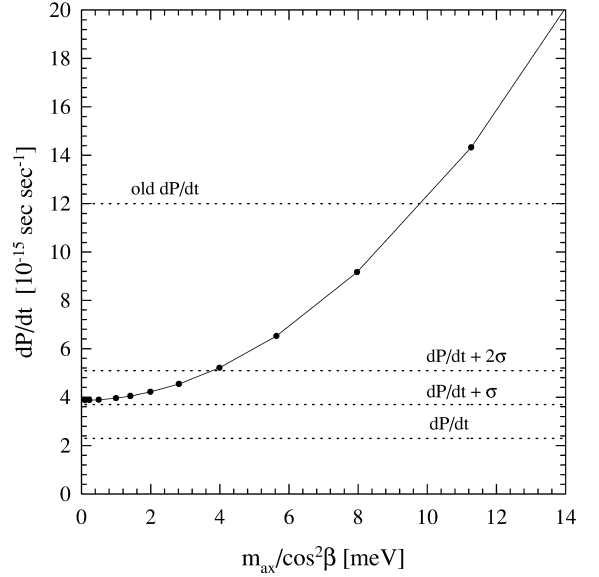


Fig. 14. The temporal derivative of the period of the $l = 1$, $k = 2$ mode of the fiducial model at $T_{\text{eff}} = 11,620$ K. The horizontal short dashed lines indicate the observed value of dP/dt , $dP/dt + \sigma$, and $dP/dt + 2\sigma$ from Kepler et al. (2000). Also, we show the old value of dP/dt value derived by Kepler et al. (1991). If we consider two standard deviations from the observational value, we conclude that the observations are compatible with an axion mass lower than $3.97 \cos^2 \beta$ meV. This is the main result of the present work.

level in our case $\dot{P}_{\text{obs}} = 5.1 \times 10^{-15} \text{ s s}^{-1}$, whereas $\dot{P}_{\text{mod}} = 3.9 \times 10^{-15} \text{ s s}^{-1}$. The observed luminosity of G117–B15A is $\log(L_{\text{phot}}/L_{\odot}) = -2.8$ (McCook and Sion, 1999). Thus, $\log(L_{\text{ax}}/L_{\odot}) \leq -3.3$. Since the axion emissivity at the relevant densities and temperatures of white dwarfs is dominated by the bremsstrahlung process, and since the degenerate core of white dwarfs, where most of bremsstrahlung processes occur, is essentially isothermal, to a very good approximation (Altherr et al., 1994) the axion luminosity is given by

$$L_{\text{ax}}/L_{\odot} \approx 2.0 \times 10^{22} g_{\text{ae}}^2 (M/M_{\odot}) (T/10^7 \text{ K})^4 \quad (9)$$

where T is the temperature of isothermal core, which for G117–B15A is typically $T \approx 1.2 \times 10^7$ K, which yields $g_{\text{ae}} \leq 1.3 \times 10^{-14}$ or, equivalently, $\approx 5 \cos^2 \beta$ meV at the 95% confidence level, which is in very good agreement with the detailed evolutionary calculations reported above.

6. Summary and conclusions

In this paper we have presented a comprehensive study of the pulsational characteristics of the variable DA white dwarf G117–B15A. This study encompasses the mode identification of the observed periods, the characterization of the structure, thickness and composition of the uppermost regions of the star, the self-consistent calculation of the evolutionary timescale and, consequently, of the rate of change of the 215.2 s period and, ultimately, the assessment of the associated uncertainties. All these required the construction of a pulsational code coupled to our previously existing evolutionary code. In this regard our results are in close agreement with the results obtained by other authors (Clemens, 1994; Bradley, 1998).

Additionally, we have used this ZZ-Ceti star to put constraints on the mass of the axion. Since G117–B15A is the most stable optical clock yet known, with a rate of the period of the 215.2 s mode of $\dot{P} = (2.3 \pm 1.4) \times 10^{-15} \text{ s s}^{-1}$ (Kepler et al., 2000), the cooling timescale of this white dwarf is well constrained. This fact has allowed us to set up tight constraints on any additional cooling mechanism different to the standard ones. Our results very much improve those previously obtained by Isern et al. (1992). In particular, we have obtained an upper bound to the mass of the axion which is $\approx 4 \cos^2 \beta \text{ meV}$ at the 95% confidence level. This upper limit is a factor of 2.5 smaller than the previously existing limits.

However, from the analysis performed in the previous sections it seems clear that in order to have more stringent upper limits to the mass of axions, we should have a smaller uncertainty in the observed value of \dot{P} , since the uncertainties in the models of white dwarf stars are clearly of lower relevance in this context. To this regard it is important to realize that at the 1σ level the stability of the dominant period of G117–B15A seems to rule out the existence of the DFSZ axion, provided that our current knowledge of the origin, structure and evolution of white dwarf stars turns out to be correct. Thus, clearly more observations are required but these observations are on their way. Since the observational situation will probably improve with the continued effort of the Whole Earth Telescope (WET) the

observational errors will decrease and, thus, there will be the possibility to set up even more tight constraints to the mass of the axion. Moreover, there are other pulsating DA white dwarfs for which an estimate of the rate of change of the period can be measured like L19-2 and R 548 (Isern et al., 1993). Although the quality of the observations is not as exceptional as those of G117–B15A it seems clear that this handful of objects could provide very valuable information and, thus, we strongly recommend continuous coverage in forthcoming WET campaigns. Finally, there are as well other — see the extensive material contained in the proceedings of the WET workshops (Meistas and Solheim, 1996; Meistas and Moskalik, 1998) — very well studied DA pulsators, being G29–38 (Kleinman et al., 1998) perhaps the best example among other ZZ-Ceti stars, for which a firm estimate of their rate of change of the period is not yet available. Thus, there are more targets to be studied which, undoubtedly, will help in improving both the theoretical and the observational situation. In any case G117–B15A seems to be a very promising stellar object to set up constraints on fundamental physics.

Acknowledgements

We would like to warmly acknowledge the comments by our anonymous referee that allowed us to improve the original version of this paper. Part of this work was supported by the Spanish DGES projects PB98-1183-C03-02, ESP98-1348 and AYA2000-1785, by the CIRIT and by Sun Microsystems under the Academic Equipment Grant AEG-7824-990325-SP.

References

- Althaus, L.G., Benvenuto, O.G., 2000. *MNRAS* 317, 952.
- Altherr, T., Petitgirard, E., Del Río Gaztelurrutia, T., 1994. *APh* 2, 175.
- Arnould, M. et al., 1999. *Nucl. Phys. A* 656, 3.
- Benvenuto, O.G., Althaus, L.G., 1998. *MNRAS* 293, 177.
- Bergström, L., 2000. *RPPH* 63, 793.
- Bergeron, P., Wesemael, F., Lamontagne, R., Fontaine, G., Saffer, R.A., Allard, N.F., 1995. *ApJ* 449, 258.
- Bradley, P.A., 1996. *ApJ* 468, 350.

- Bradley, P.A., 1998. *ApJS* 116, 307.
- Bradley, P.A., 2000, private communication.
- Bradley, P.A., Winget, D.E., Wood, M.A., 1992. *ApJ* 391, L33.
- Brassard, P., Fontaine, G., Wesemael, F., Kawaler, S.D., Tassoul, M., 1991. *ApJ* 367, 601.
- Brassard, P., Fontaine, G., Wesemael, F., Hansen, C.J., 1992. *ApJS* 80, 369.
- Brassard, P., Fontaine, G., Wesemael, F., Talon, A., 1993. In: Barstow, M.A. (Ed.), *White Dwarfs: Advances in Observations and Theory*. Kluwer Academic Publishers, Dordrecht, p. 485.
- Burrows, A., Ressel, T., Turner, M.S., 1990. *PhRvD* 42, 3297.
- Christensen-Dalsgaard, J., Mullan, D.J., 1994. *MNRAS* 270, 921.
- Carlsson, E.D., 1995. *Phys. Lett. B* 344, 245.
- Caughlan, G.R., Fowler, W.A., Harris, M.J., Zimmermann, B.A., 1985. *Atomic Data and Nuclear Data Tables* 32, 197.
- Caughlan, G.R., Fowler, W.A., 1988. *Atomic Data and Nuclear Data Tables* 40, 290.
- Clemens, J.C., 1994. PhD Thesis, University of Texas
- Córscico, A.H., Benvenuto, O.G., 2001. *Ap&SS*, in press
- Costa, J.E.S., Kepler, S.O., Winget, D.E., 1999. *ApJ* 522, 973.
- Degl'Innocenti, S., Dziembowski, W.A., Fiorentini, G., Ricci, B., 1997. *APh* 7, 77.
- Dine, M., Fischler, W., Srednicki, M., 1981. *Phys. Lett. B* 104, 199.
- Domínguez, I., Chieffi, A., Limongi, M., Straniero, A., 1999a. *ApJ* 524, 226.
- Domínguez, I., Straniero, O., Isern, J., 1999b. *MNRAS* 306, L1.
- Fontaine, G., Brassard, P., 1994. In: Chabrier, G., Schatzman, E. (Eds.), *IAU Colloq. 147, The Equation of State in Astrophysics*. Cambridge University Press, Cambridge, p. 347.
- Fontaine, G., Brassard, P., Wesemael, F., 1994. *ApJ* 428, L61.
- Hagmann, C. et al., 1998. *PhRvL* 80, 2043.
- Iben, I. Jr., 1984. *ApJ* 277, 333.
- Iben, I. Jr., MacDonald, 1985. *ApJ* 296, 540
- Isern, J., Hernanz, M., García-Berro, E., 1992. *ApJ* 392, L23.
- Isern, J., Hernanz, M., García-Berro, E., 1993. In: Barstow, M.A. (Ed.), *White Dwarfs: Advances in Observations and Theory*. Kluwer Academic Publishers, Dordrecht, p. 139.
- Keil, W., Janka, H., Schramm, D.N., Sigl, G., Turner, M.S., Ellis, J., 1997. *PhRvD* 56, 2419.
- Kepler, S.O., Robinson, E.L., Nather, R.E., McGraw, J.T., 1982. *ApJ* 254, 676.
- Kepler, S.O., Mukadam, A., Winget, D.E., Nather, R.E., Metcalfe, T.S., Reed, M.D., Kawaler, S.D., Bradley, P.A., 2000. *ApJ* 534, L185.
- Kepler, S.O. et al., 1991. *ApJ* 378, L45.
- Kepler, S.O. et al., 1995. *BaltA* 4, 221.
- Kim, J.E., 1979. *PhRvL* 43, 103.
- Kleinman, S.J., Nather, R.E., Winget, D.E., Clemens, J.C., Bradley, P.A., Kanaan, A., Provencal, J.L., Claver, C.F., Watson, T.K., Yanagida, K., Nitta, A., Dixon, J.S., Wood, M.A., Grauer, A.D., Hine, B.P., Fontaine, G., Liebert, J., Sullivan, D.J., Wickramasinghe, D.T., Achilleos, N., Marar, T.M.K., Seetha, S., Ashoka, B.N., Meistas, E., Leibowitz, E.M., Moskalik, P., Krzesinski, J., Solheim, J.E., Bruvold, A., O'Donoghue, D., Kurtz, D.W., Warner, B., Martínez, P., Vauclair, G., Dolez, N., Chevreton, M., Barstow, M.A., Kepler, S.O., Giovannini, O., Augusteijn, T., Hansen, C.J., Kawaler, S.D., 1998. *ApJ* 495, 424.
- Koester, D., Allard, N.F., 2000. *BaltA* 9, 119.
- Lazarus, D.M. et al., 1992. *PhRvL* 69, 2333.
- Magni, G., Mazzitelli, I., 1979. *A&A* 72, 134.
- Matsuki, S. et al., 1996. *Nucl. Phys. B* 51, 213.
- McCook, G.P., Sion, E.M., 1999. *ApJS* 121, 1.
- McGraw, J.T., Robinson, E.L., 1976. *ApJ* 205, L155.
- Meistas, E., Moskalik, P., 1998. *Fourth Whole Earth Telescope Workshop Proc., Baltic Astron. Ser. 7 (Vilnius: Instit. Theor. Phys. Astron.)*
- Meistas, E., Solheim, J.E., 1996. *Third Whole Earth Telescope Workshop Proc., Baltic Astron. Ser. 4 (Vilnius: Instit. Theor. Phys. Astron.)*
- Mestel, L., 1952. *MNRAS* 112, 583.
- Nakagawa, M., Kohyama, Y., Itoh, N., 1988. *ApJ* 326, 241.
- Pajdosz, G., 1995. *A&A* 295, L17.
- Peccei, R.D., Quinn, H.R., 1977. *PhRvL* 38, 1440.
- Raffelt, G.G., 1996. *Stars as Laboratories for Fundamental Physics*. University of Chicago Press, Chicago.
- Raffelt, G.G., 2000. *PhR* 333, 593.
- Raffelt, G.G., Weiss, A., 1995. *PhRvD* 51, 1495.
- Robinson, E.L., Mailloux, T.M., Zhang, E., Koester, D., Steining, R.F., Bless, R.C., Percival, J.W., Taylor, M.J., van Citters, G.W., 1995. *ApJ* 438, 908.
- Rogers, F.J., Iglesias, C.A., 1998. *SSRv* 85, 61.
- Salaris, M., Domínguez, I., García-Berro, E., Hernanz, M., Isern, J., Mochkovitch, R., 1997. *ApJ* 486, 413.
- Sikivie, P., 1983. *PhRvL* 51, 1415.
- Thielemann, F.K., Nomoto, K., Hashimoto, M.A., 1996. *ApJ* 460, 408.
- Unno, W., Osaki, Y., Ando, H., Saio, H., Shibahashi, H., 1989. *Nonradial Oscillations of Stars*. University of Tokyo Press, Tokyo.
- van Bibber, K. et al., 1994. *Int. J. Mod. Phys. Suppl. D* 3, 33.
- Woosley, S.E., Timmes, F.X., Weaver, T.A., 1993. In: Käppeler, F., Wisshak, K. (Eds.), *Nuclei in the Cosmos, Vol. 2*. IOP, Philadelphia, p. 531.